c-IAP1 and UbcH5 promote K11-linked polyubiquitination of RIP1 in TNF signalling

Jasmin N Dynek[1,3], Tatiana Goncharov[1,3], Erin C Dueber[1], Anna V Fedorova[1], Anita Izrael-Tomasevic[2], Lilian Phu[2], Elizabeth Helgason[1], Wayne J Fairbrother[1], Kurt Deshayes[1], Donald S Kirkpatrick[2] and Domagoj Vucic[1,*]

[1]Department of Protein Engineering, Genentech, Inc., South San Francisco, CA, USA and [2]Department of Protein Chemistry, Genentech, Inc., South San Francisco, CA, USA

Ubiquitin ligases are critical components of the ubiquitination process that determine substrate specificity and, in collaboration with E2 ubiquitin-conjugating enzymes, regulate the nature of polyubiquitin chains assembled on their substrates. Cellular inhibitor of apoptosis (c-IAP1 and c-IAP2) proteins are recruited to TNFR1-associated signalling complexes where they regulate receptor-stimulated NF-κB activation through their RING domain ubiquitin ligase activity. Using a directed yeast two-hybrid screen, we found several novel and previously identified E2 partners of IAP RING domains. Among these, the UbcH5 family of E2 enzymes are critical regulators of the stability of c-IAP1 protein following destabilizing stimuli such as TWEAK or CD40 signalling or IAP antagonists. We demonstrate that c-IAP1 and UbcH5 family promote K11-linked polyubiquitination of receptor-interacting protein 1 (RIP1) in vitro and in vivo. We further show that TNFα-stimulated NF-κB activation involves endogenous K11-linked ubiquitination of RIP1 within the TNFR1 signalling complex that is c-IAP1 and UbcH5 dependent. Lastly, NF-κB essential modifier efficiently binds K11-linked ubiquitin chains, suggesting that this ubiquitin linkage may have a signalling role in the activation of proliferative cellular pathways.

Introduction

The regulated modification and degradation of cellular proteins by the ubiquitin-proteasome system are critical for modulation of many vital cellular processes in both normal and tumour cells (Hershko and Ciechanover, 1998).

*Corresponding author. Department of Protein Engineering, Genentech, Inc. South San Francisco, 1 DNA Way, M/S 40, South San Francisco, CA 94080, USA. Tel.: +1 650 225 8839; Fax: +1 650 225 6127;
E-mail: domagoj@gene.com
[3]These authors contributed equally to this work

Ubiquitin, a protein whose C-terminus can be covalently linked to a lysine residue on a substrate, is instrumental in a number of cellular pathways including proinflammatory signalling, DNA damage response, and apoptosis (Hershko and Ciechanover, 1998). Ubiquitination occurs via a multistep reaction involving an E1 ubiquitin-activating enzyme, an E2 ubiquitin-conjugating enzyme, and an E3 ubiquitin ligase (Schulman and Harper, 2009). RING domain-containing ubiquitin ligases bind to both the E2 and to the substrate proteins, and mediate transfer of the ubiquitin molecule from the E2 onto a lysine residue of the substrate protein (Deshaies and Joazeiro, 2009). In cells, a single ubiquitin molecule can be covalently attached to the substrate, termed monoubiquitination, or a substrate may be modified by polyubiquitin chains, involving additional ubiquitin–ubiquitin linkages (Pickart and Fushman, 2004). Seven lysine residues in each ubiquitin molecule present an opportunity for the assembly of diverse polyubiquitin chains, with varying cellular functions (Ikeda and Dikic, 2008; Komander, 2009). While K63-linked chains are mostly implicated in proinflammatory signalling, K48-linked polyubiquitin chains predominantly target proteins for proteasomal degradation (Hershko and Ciechanover, 1998; Glickman and Ciechanover, 2002; Komander, 2009). K11-linked chains have been less studied than K48 or K63 linkages, but they seem to serve as a degradation signal for APC/C substrates in the regulation of cell division (Kirkpatrick et al, 2006; Jin et al, 2008).

Inhibitor of apoptosis (IAP) proteins are critical regulators of cellular survival capable of blocking apoptosis, modulating signal transduction, and affecting cellular proliferation (Salvesen and Duckett, 2002). In addition to their signature baculovirus IAP repeat (BIR) domains, several IAP proteins contain E3 ligase RING and ubiquitin-binding UBA domains (Vaux and Silke, 2005; Gyrd-Hansen et al, 2008; Blankenship et al, 2009). RING domain-containing cellular IAP1 and IAP2 (c-IAP1 and c-IAP2), XIAP and ML-IAP function as ubiquitin ligases that promote ubiquitination of themselves and several of their binding partners (Vaux and Silke, 2005). Cellular IAP proteins interact directly with tumour necrosis factor receptor-associated factor 2 (TRAF2), and via TRAF2, are recruited to TNF receptor-associated complexes, where they regulate apoptotic and NF-κB signalling (Rothe et al, 1995; Wang et al, 1998; Varfolomeev and Vucic, 2008). c-IAP1 and c-IAP2 are positive regulators of the TNFα-induced canonical NF-κB pathway, as they are required for receptor-interacting protein 1 (RIP1) ubiquitination and NF-κB activation (Bertrand et al, 2008; Mahoney et al, 2008; Varfolomeev et al, 2008). In the non-canonical NF-κB pathway, c-IAP proteins are negative regulators that ubiquitinate NF-κB inducing kinase (NIK), causing its proteasomal degradation and inhibition of signalling (Varfolomeev et al, 2007). RIP1 is an important link in TNFα-stimulated canonical NF-κB activation. Polyubiquitin chains assembled on RIP1 serve as a docking platform for the recruitment of the distal inhibitor of κB kinase (IKK) signalling complex, specifically the IKK subunit IKKγ, also known

as NF-κB essential modifier (NEMO) (Kovalenko and Wallach, 2006; Li et al, 2006; Scheidereit, 2006). NEMO has been reported to have a high affinity for ubiquitin chains, particularly K63-linked polyubiquitin, as opposed to mono-ubiquitin (Ea et al, 2006; Wu et al, 2006). However, recent studies have shown that K63-linked ubiquitin chains might not be absolutely essential for TNFα-stimulated NF-κB activation, and that NEMO also possesses high affinity for other ubiquitin chains (Lo et al, 2009; Rahighi et al, 2009; Xu et al, 2009).

There are over 30 human E2 ubiquitin-conjugating enzymes and possibly hundreds of E3 ubiquitin ligases. Thus, one can appreciate the degree of substrate specificity and ubiquitin chain variability that is potentially imparted by E2–E3 pairs. A previous study that interrogated E2–E3 interactions by a yeast two-hybrid strategy yielded insight into how specific ubiquitin modifications are generated by individual E2–E3 interactions (Christensen et al, 2007). Here, we describe a directed yeast two-hybrid screen that identified both novel and previously known E2 partners of IAP RING domains. Our results show that E2 enzymes of the UbcH5 family are critical functional partners for the E3 ligase activity of c-IAP proteins. Downregulation of UbcH5a/b/c levels restored c-IAP1 protein levels following destabilizing stimuli such as IAP antagonists or TWEAK or CD40 signalling, and prevented degradation of the c-IAP substrate NIK. In addition, we demonstrate that c-IAP1 and UbcH5 family promote K11-linked polyubiquitination of RIP1. Using ubiquitin linkage-specific antibodies, we show that TNFα-stimulated NF-κB activation involves K11-linked ubiquitination of RIP1 within the TNFR1 signalling complex, which is dependent on c-IAP1 and UbcH5. Finally, we provide evidence that the adaptor protein NEMO can bind K11 ubiquitin chains, indicating that this ubiquitin linkage may have a non-degradative signalling role in the activation of proliferative cellular pathways.

Results

Identification of interactions between IAP RING domains and E2 ubiquitin-conjugating enzymes

IAP proteins c-IAP1, c-IAP2, ML-IAP, and XIAP are RING domain-containing ubiquitin ligases that promote assembly of polyubiquitin chains both on themselves and on several signalling molecules (Vaux and Silke, 2005; Varfolomeev and Vucic, 2008). To further elucidate the mechanism of ubiquitination mediated by IAP proteins, we examined interactions between IAP RING domains and E2 ubiquitin-conjugating enzymes in a series of directed yeast two-hybrid screens. We used individual c-IAP1, c-IAP2, ML-IAP, and XIAP RING domain constructs as baits against a library of 30 human E2 prey constructs. In total, 120 interactions were tested (Supplementary Figure S1). Positive and negative controls, including interactions of a BRCA1 RING–BARD1 RING fusion and UbcH5b/c, were assayed to validate the screen (Christensen et al, 2007) (Supplementary Figure S2). A number of E2 partners were shared amongst the IAP RING domains tested, while other E2 interactions were specific to particular IAP RING domains (Figure 1A; Supplementary Figure S1).

The three isoforms of the UbcH5 family of E2 enzymes (UbcH5a, UbcH5b, and UbcH5c) were found to interact with all IAP RING domains tested, consistent with published *in vitro* binding and ubiquitination assay studies (Figure 1A)

(Yang and Du, 2004; Mace et al, 2008; Varfolomeev et al, 2008). The RING domain of c-IAP1 specifically interacted with tsg101, Ube2s, and Rad6b, while Ube2Q2 interacted with the RING domains of c-IAP1 and c-IAP2, but not with those of ML-IAP or XIAP (Figure 1A). On the other hand, ML-IAP and XIAP RING domains interacted with UbcH6, again consistent with published *in vitro* ubiquitination assay results (Yang and Du, 2004). Although UbcH13 has been reported to function as an E2 in combination with c-IAP in *in vitro* ubiquitination assays (Bertrand et al, 2008), interactions were not observed between UbcH13 and any of the IAP RING family members tested (Supplementary Figure S1). This finding is consistent with our previously published *in vitro* ubiquitination assay data (Varfolomeev et al, 2008). To further verify this result, the UbcH13 construct was functionally validated in yeast two-hybrid assays with TRAF2 and TRAF6 RING domains. As previously reported (Yin et al, 2009a, b), TRAF6 RING domain bound UbcH13, while no interaction was observed between TRAF2 RING and UbcH13 (Supplementary Figure S2).

In order to further validate the IAP RING domain interactions with the UbcH5 family, we made mutations in the IAP RING bait constructs that are predicted to disrupt the RING domain's E2-binding surface or to prevent dimerization (Figure 1B and C) (Mace et al, 2008). In agreement with the reported structural studies, we found that the c-IAP2 V559A E2-binding surface mutant lost the ability to interact with UbcH5b. However, it retained the ability to dimerize, as assayed by interaction with a wild-type c-IAP2 RING prey construct (Figure 1B). On the other hand, the c-IAP2 F602A dimerization mutant failed to interact with UbcH5b and was unable to dimerize with the wild-type c-IAP2 RING domain. The c-IAP1, ML-IAP, and XIAP E2-binding surface mutations also abrogated interactions with UbcH5b, and, except in the case of XIAP RING I452A, had no effect on RING domain dimerization. Predicted dimerization mutations in c-IAP1, ML-IAP, and XIAP RING domains prevented their interaction with the corresponding wild-type IAP RING domain constructs. The ML-IAP RING F296A dimerization mutant did not interact with UbcH5b, but the c-IAP1 and XIAP dimerization mutants supported interactions with UbcH5b (Figure 1B). Additionally, mutations of the predicted E2 binding and RING domain dimerization residues in c-IAP1 and ML-IAP RING domains prevented their interactions with several other E2 enzymes identified as potential IAP-interacting partners from the initial yeast two-hybrid screen (Supplementary Figure S3A and B). We also tested the Ubc9 interactions in an analogous manner and concluded that the observed Ubc9 interactions (Figure 1A) were most likely non-specific, as none of the mutations tested affected interaction with Ubc9 (Supplementary Figure S3C). In sum, our directed yeast two-hybrid screens confirmed several known interactions and also identified a number of novel interactions, between the IAP RING domains and E2 enzymes, thereby providing a more thorough understanding of IAP-mediated ubiquitination.

Ube2S promotes ubiquitin chain extension in combination with c-IAP1 and UbcH5a

Having identified Ube2S as a binding partner of the c-IAP1 RING domain in a directed yeast two-hybrid screen, we wanted to investigate whether this E2 enzyme can work with the E3 ligase c-IAP1 to promote ubiquitin chain
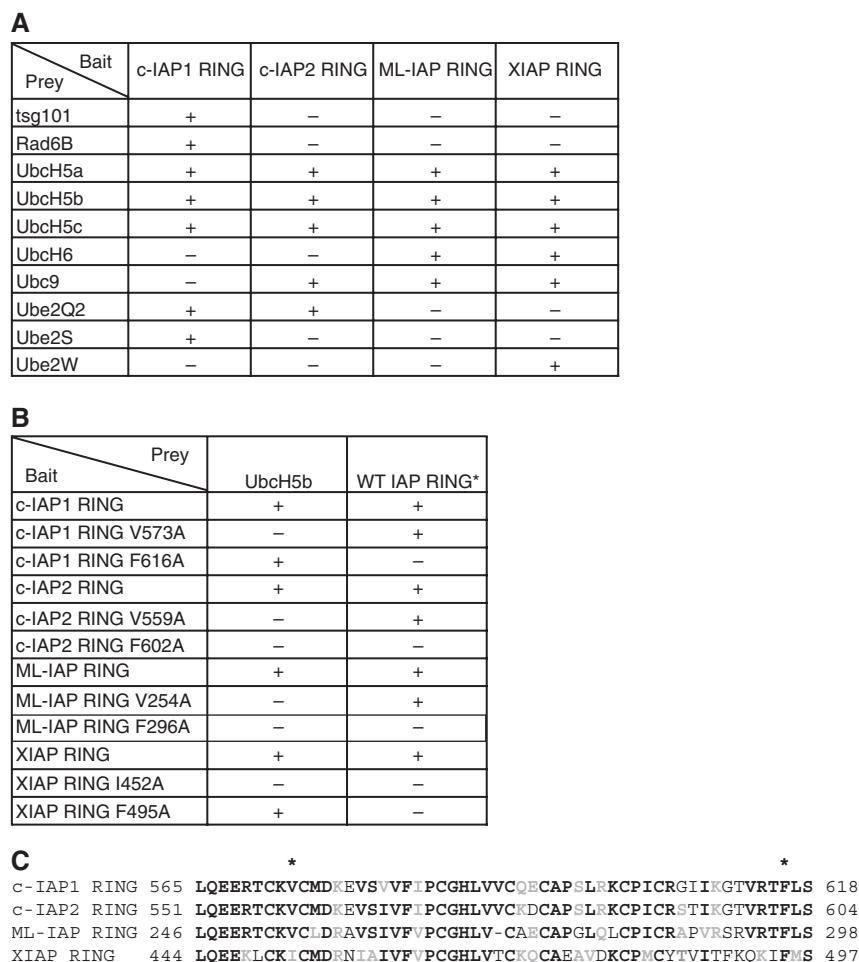
A

Prey \ Bait	c-IAP1 RING	c-IAP2 RING	ML-IAP RING	XIAP RING
tsg101	+	−	−	−
Rad6B	+	−	−	−
UbcH5a	+	+	+	+
UbcH5b	+	+	+	+
UbcH5c	+	+	+	+
UbcH6	−	−	+	+
Ubc9	−	+	+	+
Ube2Q2	+	+	−	−
Ube2S	+	−	−	−
Ube2W	−	−	−	+

B

Bait \ Prey	UbcH5b	WT IAP RING*
c-IAP1 RING	+	+
c-IAP1 RING V573A	−	+
c-IAP1 RING F616A	+	−
c-IAP2 RING	+	+
c-IAP2 RING V559A	−	+
c-IAP2 RING F602A	−	−
ML-IAP RING	+	+
ML-IAP RING V254A	−	+
ML-IAP RING F296A	−	−
XIAP RING	+	+
XIAP RING I452A	−	−
XIAP RING F495A	+	−

C

```
                          *                                              *
c-IAP1 RING 565 LQEERTCKVCMDKEVSVVFIPCGHLVVCQECAPSLRKCPICRGIIKGTVRTFLS 618
c-IAP2 RING 551 LQEERTCKVCMDKEVSIVFIPCGHLVVCKDCAPSLRKCPICRSTIKGTVRTFLS 604
ML-IAP RING 246 LQEERTCKVCLDRAVSIVFVPCGHLV-CAECAPGLQLCPICRAPVRSRVRTFLS 298
XIAP RING   444 LQEEKLCKICMDRNIAIVFVPCGHLVTCKQCAEAVDKCPMCYTVITFKQKIFMS 497
```

Figure 1 IAP RING domain constructs interact with E2 ubiquitin-conjugating enzymes by yeast two-hybrid analysis. (**A**) Summary of positive interactions for each IAP RING domain DNA-binding fusion bait construct (c-IAP1 RING, c-IAP2 RING, ML-IAP RING, XIAP RING) with E2 activation domain fusion prey constructs. Interactions were scored according to growth on selective medium; + indicates growth present; − indicates growth absent. (**B**) Summary of interactions for UbcH5b and wild-type IAP RING domain prey constructs with wild-type IAP RING, IAP RING E2-binding surface mutants (c-IAP1 RING V573A, c-IAP2 RING V559A, ML-IAP RING V254A, XIAP RING I452A), and IAP RING dimerization mutants (c-IAP1 RING F616A, c-IAP2 RING F602A, ML-IAP RING F296A, XIAP RING 495A) bait constructs. WT IAP RING* denotes that the respective wild-type IAP RING prey constructs were tested for each set of interactions (for instance, wild-type c-IAP1 RING prey and c-IAP1 RING F616A bait). (**C**) Sequence alignment of IAP RING domains, bold black type indicates amino acid residues with conserved identities, bold grey type indicates amino acid residues with conserved side chain properties, and asterisks mark the locations of E2-binding surface and dimerization residues mutated in the IAP RING bait constructs.

formation. Initial attempts using a standard ubiquitination protocol with Ube2S and c-IAP1, together with an E1 enzyme and an energy source, did not yield any ubiquitin chains at several different temperatures (17–37°C) and reaction times (30 min to 2 h) (Figure 2A and B). At the same time, UbcH5a in combination with c-IAP1 efficiently formed polyubiquitin chains. This validates the other components of the reaction, including the recombinant c-IAP1 protein (Figure 2A and B). Recent reports on the enzymatic activity of Ube2S indicate that this E2 enzyme can extend the ubiquitin chains initiated by other E2 enzymes, such as UbcH10 (Garnett *et al*, 2009; Williamson *et al*, 2009). Thus, we modified the reactions to include a 5-min preincubation of c-IAP1 with 5% of the UbcH5a concentration used in UbcH5a control reactions as a first step, which did not promote significant c-IAP1 auto-ubiquitination. Following that first step, the E2 enzymes UbcH5a or Ube2S were added, and these second-step reactions were allowed to proceed for another 35 min. This experimental design revealed ubiquitination activity and demonstrated the ability of Ube2S to promote ubiquitin

chain assembly in conjunction with UbcH5a (Figure 2). Ubiquitination reactions were quantified using the ubiquitin-AQUA method (Kirkpatrick *et al*, 2006; Blankenship *et al*, 2009). Equivalent gel regions from each sample were excised from the Coomassie blue-stained SDS–PAGE gel, beginning above the unmodified c-IAP1 bands (Figure 2A). Quantification of the ubiquitin reactions confirmed the results obtained using an anti-ubiquitin antibody in western blotting, and demonstrated the ability of Ube2S to promote ubiquitin chain assembly (Figure 2C; Supplementary Figure S4). Thus, Ube2S can act as a functional partner of c-IAP1 to promote the assembly of polyubiquitin chains in combination with another E2 enzyme, namely UbcH5a.

The UbcH5 family of E2 enzymes regulates the stability of c-IAP1 and the c-IAP substrate NIK

We next focussed on the c-IAP1 E2 interactions, both those shared amongst IAP family members and those specific to c-IAP1, to investigate their physiological impact on the stability of c-IAP1 protein and its substrates in human cancer
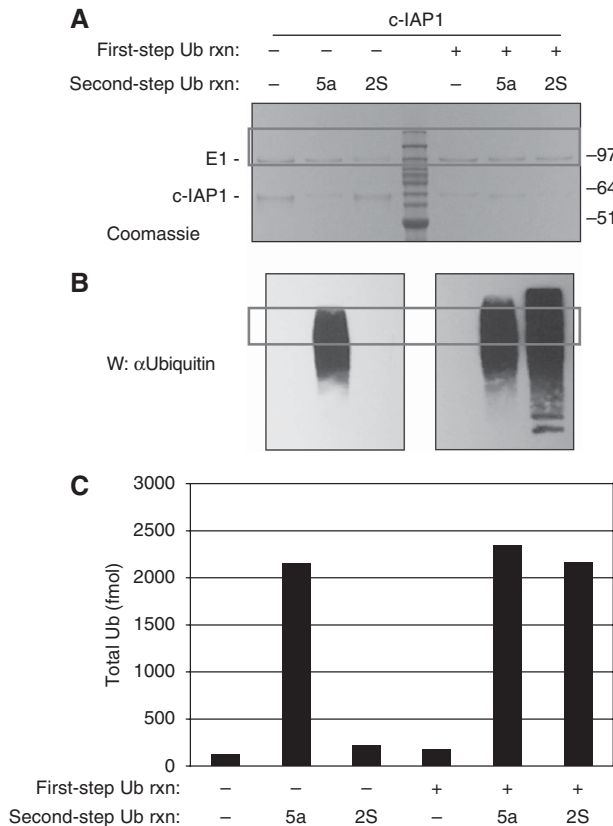
Figure 2 Ube2S can promote ubiquitin chain extension in combination with c-IAP1 and UbcH5a. (**A**) Coomassie-stained gel containing equivalent amounts of *in vitro* c-IAP1 autoubiquitination reactions (rxn) performed in two steps with the first-step reaction conducted in the absence or the presence of UbcH5a as described in Materials and methods. The red boxes mark the boundaries of gel regions that were excised and subjected to in-gel trypsin digestion, followed by Ubiquitin-AQUA analysis. (**B**) Western blot using anti-ubiquitin antibody (P4D1) of autoubiquitination reactions. (**C**) Quantification of the amount of total ubiquitin in each corresponding gel region for each sample. A full-colour version of this figure is available at *The EMBO Journal* Online.

cells. To this end, we transiently transfected HKB11 cells stably expressing the human CD40 receptor (HKB11-CD40) with siRNAs targeting the c-IAP1-interacting E2 enzymes. Treatment of HKB11 cells with anti-CD40 antibody resulted in a decrease in c-IAP1 protein levels, as seen in control siRNA-transfected cells (Figure 3A). Knockdown of the UbcH5 family of E2 enzymes stabilized c-IAP1 protein levels following CD40 stimulation (Figure 3A, top left panel), while no changes in c-IAP1 protein levels were observed with siRNA knockdowns of Ube2S, tsg101, Ube2Q2, or Rad 6B (Figure 3A; Supplementary Table I). The stability of XIAP was not affected by CD40 treatment while c-IAP2 or ML-IAP expression could not be detected in these cells (Supplementary Figure S5A). The IAP antagonist MV1 stimulates the E3 ligase activity and autoubiquitination of c-IAP1 (Varfolomeev *et al*, 2007). However, c-IAP1 protein levels were stabilized in cells transfected with UbcH5 siRNA following MV1 treatment (Supplementary Figure S5B). We also analysed the role of UbcH5 proteins in signalling by the TNF superfamily ligand, TWEAK. Downregulation of UbcH5 family expression, but not Ube2S expression, stabilized c-IAP1 protein levels following TWEAK treatment (Figure 3B). In addition, UbcH5

knockdown significantly blunted stimulation of gene expression by TWEAK and TNFα (Figure 3C; Supplementary Figure S6), suggesting that the UbcH5 family of E2 enzymes has an important role in these TNF ligands-mediated signalling pathways.

NIK is a substrate of the E3 ligases c-IAP1 and c-IAP2 in the non-canonical NF-κB signalling pathway (Varfolomeev *et al*, 2007; Vince *et al*, 2007). In order to examine which E2 enzyme acts in concert with the c-IAP proteins to regulate NIK stability we co-expressed myc-NIK and FLAG-c-IAP1, FLAG-c-IAP2, or FLAG-vector in 293T cells, in combination with transfections of siRNA targeting the c-IAP1-interacting E2 enzymes. NIK protein levels decreased drastically upon co-expression with either c-IAP1 or c-IAP2, as shown previously (Varfolomeev *et al*, 2007). However, siRNA knockdown of the UbcH5 family greatly increased NIK protein levels in cells overexpressing c-IAP1 or c-IAP2 (Figure 3D, left panel). NIK protein levels were largely unchanged when any of the other c-IAP1-interacting E2 enzymes were silenced via siRNA (Figure 3D; Supplementary Table II). In addition, E2 binding and RING dimerization mutants of c-IAP1 were unable to promote NIK degradation, while the co-expression of siRNA-resistant UbcH5b construct reversed the effect of UbcH5 knockdown on NIK stability (Supplementary Figure S7A and B). Collectively, these results suggest that the UbcH5 family of E2 enzymes regulates the stability of both c-IAP1 protein and its substrates in response to cellular signalling.

c-IAP1 promotes K11 polyubiquitin linkage formation on RIP1

Another important substrate of the c-IAP proteins is the Ser/Thr kinase RIP1, a critical mediator of TNFα-stimulated canonical NF-κB signalling (Varfolomeev and Vucic, 2008). Cellular IAP proteins can promote K48- and K63-linked polyubiquitination of RIP1 (Bertrand *et al*, 2008; Varfolomeev *et al*, 2008), but whether RIP1 can be modified by other ubiquitin linkages is not clear. Given that c-IAP1 autoubiquitination generates significant levels of K11 linkages *in vitro* (Blankenship *et al*, 2009) and that the c-IAP1 RING domain interacts with the K11 linkage-promoting E2 enzymes UbcH5 and Ube2s, we examined whether c-IAP1 can promote addition of K11 linkages to RIP1. First, we demonstrated that c-IAP1 is capable of mediating K11-linked polyubiquitination on itself and RIP1. Transfection of 293T cells with c-IAP1, RIP1 and wild-type or K11-, K48-, or K63-only ubiquitin mutants, followed by lysis under denaturing conditions and immunoprecipitation showed that c-IAP1 and RIP1 can carry K11 linkages *in vivo* (Figure 4A). On the other hand, the E2 binding and RING dimerization mutants of c-IAP1 failed to promote RIP1 ubiquitination in 293T cells or c-IAP1-deficient MEF cells (Supplementary Figure S8A and B). Reconstituted ubiquitination reactions with recombinant proteins demonstrated the K11-linked polyubiquitination of c-IAP1 and RIP1 *in vitro* in combination with UbcH5 a, b, or c variants and with K11R, K48R, or K63R ubiquitin proteins as well as with Ube2S in a two-step reaction (Figure 4B; Supplementary Figure S8C–E). The closely related c-IAP2 protein was also capable of mediating K11-linked polyubiquitination of itself and of RIP1 (Supplementary Figure S9).

Next, we further explored whether c-IAP1 could promote K11-linked RIP1 ubiquitination using quantitative mass spectrometry. To accomplish this, *in vitro* reconstituted
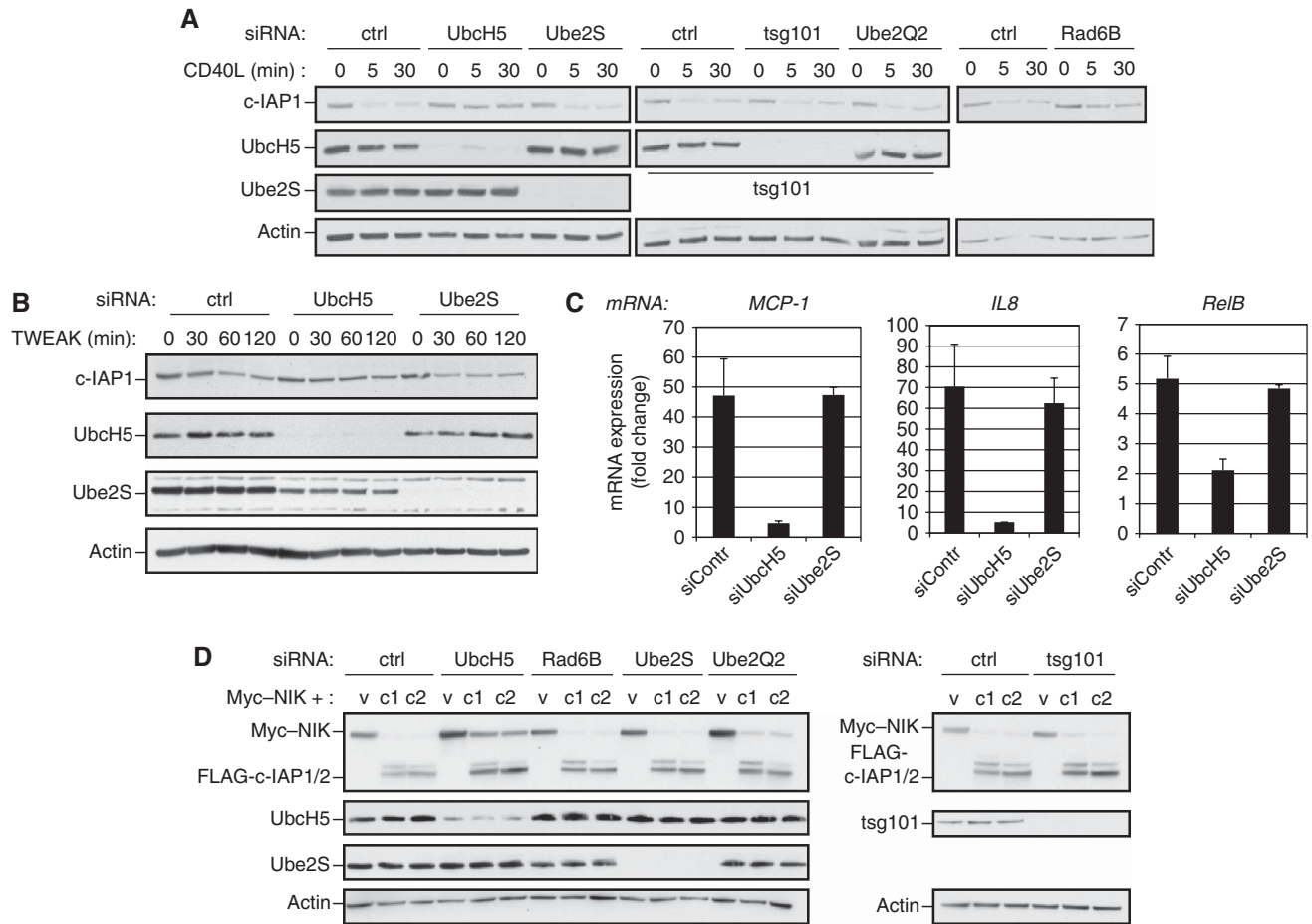
Figure 3 siRNA knockdown of the UbcH5 family increases the stability of c-IAP1 and the c-IAP1 substrate NIK. (**A**) siRNA-mediated knockdown of the UbcH5 family of E2 enzymes increases c-IAP1 protein levels following CD40 treatment. HKB11-CD40 cells were transfected with control siRNA, or siRNA targeting the UbcH5 family (UbcH5a, UbcH5b, UbcH5c isoforms), Ube2S, tsg101, Ube2Q2, or Rad6B for 48 h. Anti-CD40 antibody was cross-linked with secondary antibody for 10 min, and then added to cells at a concentration of 0.5 μg/ml for 0, 5, or 30 min. Lysates were collected and subjected to western blot analysis using antibodies for detection of c-IAP1, UbcH5 (the antibody recognizes all three isoforms), tsg101, and actin, as a loading control. In parallel, RNA samples were collected and purified to monitor the efficiency of Ube2Q2 and Rad6B siRNA-knockdown by quantative RT–PCR analysis (Supplementary Table I). (**B**) siRNA-mediated knockdown of the UbcH5 family of E2 enzymes increases c-IAP1 protein levels following TWEAK treatment. HT1080 cells were transfected with control siRNA, or siRNA targeting the UbcH5 family (UbcH5a, UbcH5b, UbcH5c isoforms), or Ube2S for 48 h and then treated with TWEAK (100 ng/ml) for indicated time points. Lysates were collected and subjected to western blot analysis using antibodies for detection of c-IAP1, UbcH5 (the antibody recognizes all three isoforms), Ube2S, and actin, as a loading control. (**C**) Knockdown of UbcH5 family inhibits gene induction by TWEAK. HT1080 cells were treated with TWEAK for 4 h (or 7 h for *RelB*), and RNA samples from treated and untreated cells were analysed by quantitative real-time PCR analysis. All values were normalized to an *RPL19* RNA internal control. Columns represent mean from triplicate experiments and bars represent s.d. (**D**) siRNA-mediated knockdown of the UbcH5 family of E2 enzymes increases NIK protein stability in the presence of the c-IAP proteins. HEK293T cells were transfected with control siRNA, or siRNA targeting the UbcH5 family, Ube2S, tsg101, Ube2Q2, or Rad6B. At 24 h later, cells were transfected with myc-NIK1 plus FLAG-c-IAP1, FLAG-c-IAP2, or FLAG-vector. The following day, lysates were collected and analysed by western blot, and RNA was prepared for quantitative RT–PCR analysis (Supplementary Table II) as in panel (**A**).

ubiquitination reactions including c-IAP1, RIP1, and UbcH5a were denatured in 6 M urea, followed by immunoprecipitation with anti-RIP1 antibody from diluted protein samples. Western blot analysis of this reaction mixture showed that the absence of urea allowed detection of c-IAP1 in the immunoprecipitated protein complex, while the presence of the denaturing agent eliminated c-IAP1 from the precipitates (Figure 4C; Supplementary Figure S10A). At the same time, elimination of c-IAP1 from the immunoprecipitates did not affect RIP1-conjugated ubiquitination, as shown by western blotting with an anti-ubiquitin antibody (Supplementary Figure S10A). Using this experimental design we analysed equivalent gel regions from samples that did, or did not, contain ubiquitinated RIP1 (Figure 4C). Mass spectrometry

analysis revealed the presence of RIP1, and absence of c-IAP1 proteins, in the RIP1-containing sample (Figure 4C; Supplementary Figure S10B). Subsequent analyses of the ubiquitination reactions using the ubiquitin-AQUA method demonstrated the presence of ubiquitin and, importantly, K11-linked ubiquitin chains in the RIP1-containing sample (Figure 4C, top and bottom panels). Therefore, our *in vivo* and *in vitro* studies establish clearly that c-IAP1 can promote K11-linked polyubiquitination of RIP1.

TNF signalling stimulates c-IAP1 and UbcH5-dependent K11-linked polyubiquitination of RIP1
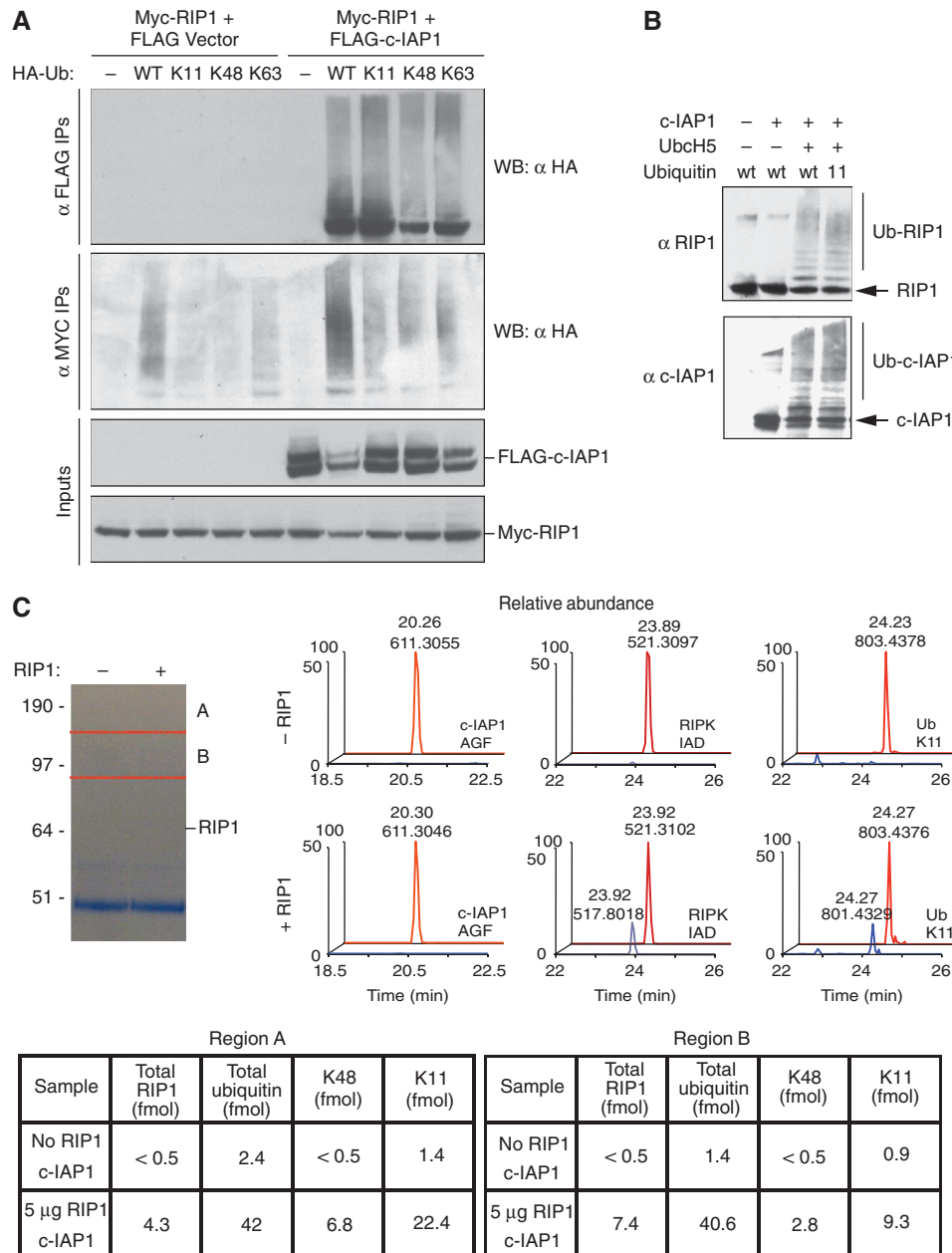During TNFα signalling, RIP1 is recruited to the TNFR1 complex and subject to polyubiquitination by c-IAP1

Region A					Region B				
Sample	Total RIP1 (fmol)	Total ubiquitin (fmol)	K48 (fmol)	K11 (fmol)	Sample	Total RIP1 (fmol)	Total ubiquitin (fmol)	K48 (fmol)	K11 (fmol)
No RIP1 c-IAP1	< 0.5	2.4	< 0.5	1.4	No RIP1 c-IAP1	< 0.5	1.4	< 0.5	0.9
5 µg RIP1 c-IAP1	4.3	42	6.8	22.4	5 µg RIP1 c-IAP1	7.4	40.6	2.8	9.3

Figure 4 c-IAP1 promotes K11 polyubiquitin linkage formation on RIP1. (**A**) Ectopic expression of c-IAP1 and RIP1 promotes K11-linked polyubiquitination in 293T cells. HEK293T cells were transfected with myc-RIP1, HA-tagged ubiquitin constructs (WT, K11-, K48-, or K63-only), with or without Flag-c-IAP1 for 24 h. Cells were pretreated with MG132 (20 µM) for 1 h, lysates were boiled in NP40 lysis buffer containing 1% SDS for 10 min, diluted 10-fold and immunoprecipitated using anti-myc or anti-Flag beads. Flag c-IAP1 and myc-RIP1 were detected in immunoprecipitated material and in input lysates using anti-HA, anti-myc, and anti-Flag antibodies. (**B**) Recombinant RIP1 was incubated for 45 min in a ubiquitination reaction in the absence or the presence of recombinant c-IAP1, UbcH5a, and wild-type or K11-only ubiquitin proteins. RIP1 and c-IAP1 modifications were determined with anti-RIP1 and anti-c-IAP1 antibodies. (**C**) Determination of c-IAP1-mediated polyubiquitin linkages on RIP1. Recombinant RIP1 (5 µg) was incubated for 45 min in ubiquitination reactions in the presence of recombinant c-IAP1 (1.25 µg), UbcH5a (1.25 µg), and wild-type ubiquitin. Following ubiquitination reactions, samples were incubated in 6 M Urea at room temperature for 30 min with rocking, diluted 15 times and immunoprecipitated using anti-RIP1 antibodies. Coomassie-stained gel containing equivalent amounts of immunoprecipitated RIP1 (left side): the red lines mark the boundaries of gel regions that were excised and subjected to in-gel trypsin digestion, followed by Ubiquitin-AQUA analysis using OrbiTrap (bottom and right). Extracted ion chromatograms of indicated peptides from gel region A are shown where heavy peaks (red), corresponding to isotope labelled internal standard peptides, and light peaks (blue), corresponding to digested analyte peptides, are labelled with retention time and *m/z* ratio. The relative abundance for light peptide chromatograms (*y* axis) has been zoomed 2X relative to corresponding heavy peptides. Quantification of the amount of c-IAP1, RIP1 protein, total ubiquitin, and K11-linked ubiquitin for each corresponding gel region for each sample is shown on the bottom.

(Bertrand *et al*, 2008; Varfolomeev *et al*, 2008). To date, TNFR1-bound RIP1 has been demonstrated to be modified by both K48- and K63-linked polyubiquitin chains (Newton

et al, 2008). Given that we detected a significant amount of K11-linked polyubiquitin chains on RIP1 generated by *in vitro* ubiquitination assays (Figure 4B and C), we hypothesized

that TNFα-induced ubiquitination of RIP1 may also include K11-linked polyubiquitin chains. To explore this possibility, HT29 cells were treated with TNFα, and the denatured cellular lysates were immunoprecipitated with the recently described K11-, K48-, or K63-linkage-specific anti-ubiquitin antibodies (Supplementary Figure S11A) (Newton *et al*, 2008; Matsumoto *et al*, 2010). Western blotting with anti-RIP1 antibody showed a significant amount of RIP1 in the K11- and K63-immunoprecipitated material (Supplementary Figure S11A). To further investigate if RIP1 is modified by K11-linked ubiquitin chains within the TNFR1 complex, HeLa S3 cells were treated with TNFα, and TNFR1-associated proteins were immunoprecipitated with anti-TNFR1 antibodies. Next, the receptor complexes were disassociated under denaturing conditions, and secondary immunoprecipitations using K11-, K48-, or K63-linkage-specific anti-ubiquitin antibodies were performed, followed by western blot analysis to detect ubiquitinated RIP1. Immunoprecipitation with the K11-linkage-specific anti-ubiquitin antibody revealed that a significant amount of TNFR1-bound RIP1 was modified by K11-linked polyubiquitin chains following TNFα stimulation, similar to the amount of TNFR1-bound RIP1 that was immuno-precipitated with the K63-linkage-specific anti-ubiquitin antibody (Figure 5A). RIP1 K11-linked polyubiquitination peaked at early time points following TNFα stimulation, and decreased with longer treatments (Figure 5B). As K11-linked polyubiquitination has been reported in conjunction with protein degradation, we explored whether TNFα-stimulated K11-linked polyubiquitination affects the stability of RIP1 (Supplementary Figure S11B and C). Pretreatment of cells with the proteasome inhibitor MG132 did not affect the RIP1 levels in cellular lysates or in K11 linkage-associated immunoprecipitates from TNFα-stimulated cells (Supplementary Figure S11B). However, pretreatment with MG132 increased the levels of TNFR1-associated K11-ubiquitinated RIP1, suggesting that a portion of the K11 linkage-modified RIP1 might be degraded (Supplementary Figure S11C).

We have previously shown that TNFα-stimulated RIP1 polyubiquitination is mediated by c-IAP proteins (Varfolomeev *et al*, 2008), and therefore RIP1 K11-linked polyubiquitination may also depend on c-IAP1 and c-IAP2. In order to deplete c-IAP proteins prior to stimulating with TNFα, HeLa S3 cells were treated for 16 h with the IAP antagonist BV6, resulting in a marked reduction in c-IAP1 protein levels (Figure 5C, left panel). Loss of c-IAP1 substantially reduced K11-, K48-, and K63-linked polyubiquitination of RIP1 (Figure 5C, right panel). Along with the mass spectrometry data, these results indicate that c-IAP1 can act as an E3 ligase to promote TNFα-induced K11-linked polyubiquitination of RIP1 in the TNFR1 complex. Furthermore, siRNA-mediated knockdown of the UbcH5 family of E2 enzymes, but not of UbcH13 or Ube2S, decreased the amount of K11-linked polyubiquitinated RIP1 immunoprecipitated under denaturing conditions from HeLa S3 cells (Figure 5D). Taken together, these data suggest that the UbcH5 family of E2 enzymes acts with the E3 ligase c-IAP1 to facilitate K11-linked polyubiquitination of RIP1 in TNFα signalling.

NEMO binds K11-linked ubiquitin chains
TNFα-induced activation of canonical NF-κB signalling requires the ubiquitin-binding protein NEMO as a critical link in the activation of the IKK kinase complex and the subsequent phosphorylation and degradation of IκB. As binding of NEMO to polyubiquitin chains assembled on RIP1 is crucial for its engagement in the TNFR1 complex, we investigated if NEMO could bind K11-linked ubiquitin chains. To that end, we developed a binding assay based on biolayer interferometry. N-terminal His$_6$-Avi-tagged constructs containing the ubiquitin-binding domain of NEMO (NEMO$_{UBD}$) and the ubiquitin-binding region c-IAP1, which includes its UBA domain (c-IAP1$_{BIR3-RING}$), were expressed in *Escherichia coli* cells with biotin ligase to generate site-specifically biotinylated protein stocks. We then loaded bio-tinylated NEMO$_{UBD}$ or c-IAP1$_{BIR3-RING}$ onto streptavidin bio-sensors and transferred the sensor tips into ubiquitin dimer stocks of various concentrations and linkage types or ubiquitin monomer. For all cases, we observed direct binding that rapidly reached saturation (Figure 6A) and, as such, we performed equilibrium-binding analysis to quantify the interactions (Figure 6B). The determined K_d values are summarized in Figure 6C.

As previously reported, NEMO$_{UBD}$ displayed preferential binding to linear ubiquitin dimer ($K_d = 1.1 \pm 0.2\,\mu M$) over the other chain linkages while showing no significant binding to monomeric ubiquitin ($K_d > 90\,\mu M$) (Lo *et al*, 2009; Rahighi *et al*, 2009). We observed substantial binding of NEMO$_{UBD}$ to K11-, K48-, and K63-linked ubiquitin dimers, with similar affinities for these dimer linkages. Furthermore, association of NEMO with K11- and K63-linked polyubiquitin chains *in vivo* and in a TNF stimulus-dependent manner was also observed (Figure 6D; Supplementary Figure S12). As a comparison, we tested the c-IAP1$_{BIR3-RING}$ construct and found that it bound to all ubiquitin chains with approximately equivalent affinity ($K_d \sim 1$–$3\,\mu M$). Binding of c-IAP1$_{BIR3-RING}$ to ubiquitin monomer ($K_d = 18.5 \pm 4.9\,\mu M$), as well as K48- and K63-linked ubiquitin chains, was similar to that observed in earlier studies that used the c-IAP1 UBA domain only (Blankenship *et al*, 2009). In conclusion, these results indicate strongly that K11-linked ubiquitin chains can serve as a molecular signal for recruitment of NEMO and participate in TNF signalling.

Discussion

The assembly of polyubiquitin chains is a carefully orchestrated process, during which ubiquitin ligases and ubiquitin-conjugating enzymes cooperatively modify their substrates with diverse ubiquitin linkages (Ikeda and Dikic, 2008). While ubiquitin ligases determine the substrate specificity, E2 ubiquitin-conjugating enzymes provide the capacity for building various ubiquitin linkages. To identify E2-binding partners of IAP RING domains, we used a directed yeast two-hybrid assay. This approach confirmed several known interactions and also identified a number of novel IAP RING domain-binding E2 enzymes. In line with previously reported structural and functional studies, the UbcH5 family of E2 enzymes bound the RING domains of c-IAP1, c-IAP2, ML-IAP, and XIAP. Mutations in the predicted E2-binding surface of the IAP RING domains, based on the published crystal structure of UbcH5b and c-IAP2 RING domain homo-dimer (Mace *et al*, 2008), abolished the UbcH5b interactions for all IAP RING constructs tested. For the most part, the E2-binding surface mutations did not interfere with IAP RING domain dimerization, and thus are unlikely to have affected
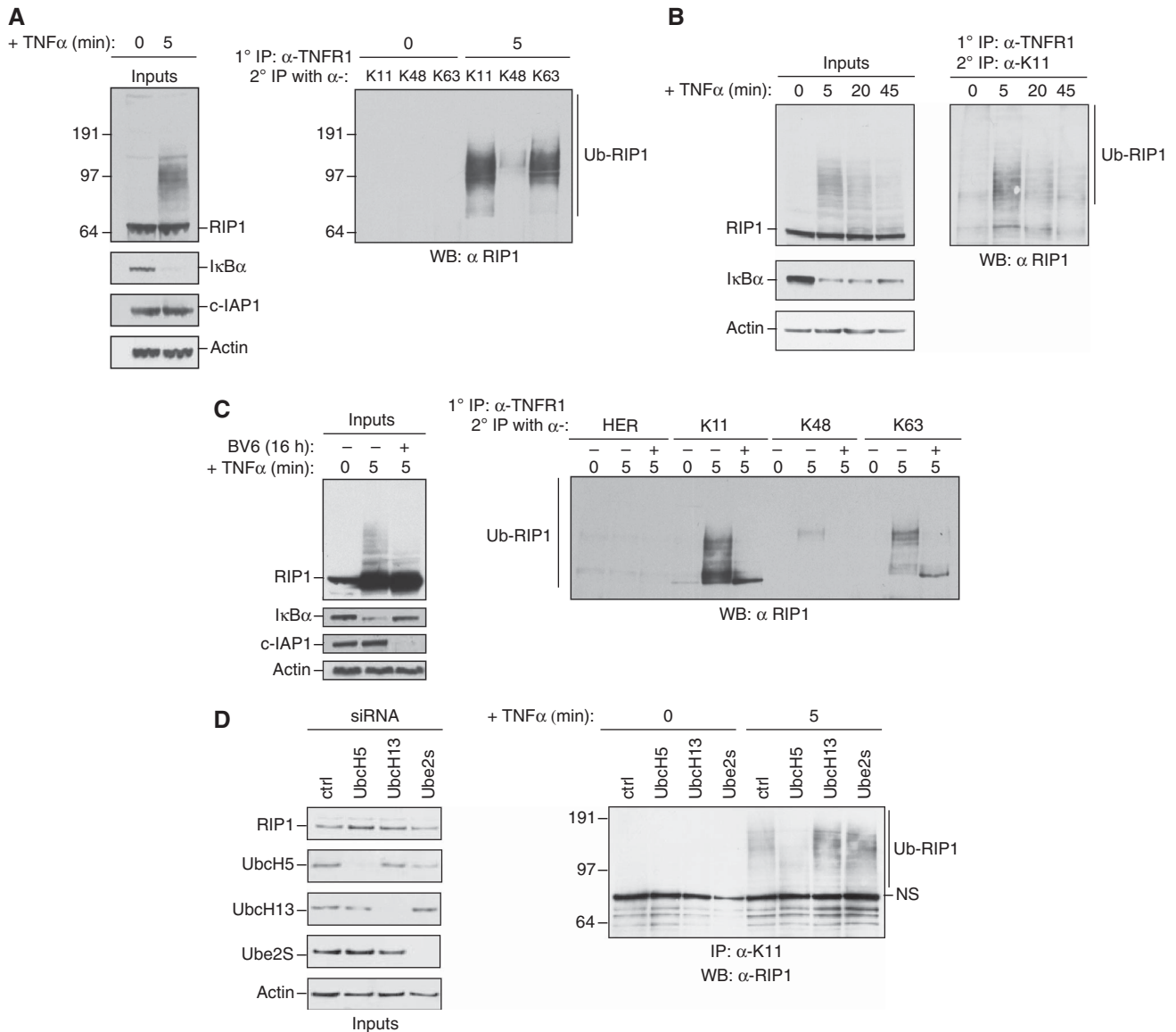
Figure 5 TNF signalling stimulates K11-linked polyubiquitination of RIP1 by c-IAP1 and UbcH5. (**A**) TNFR1-bound RIP1 undergoes K11-linked polyubiquitination in response to TNFα. HeLa S3 cells were pretreated with 20 μM MG132 for 10 min, and then incubated with or without 100 ng/ml TNFα for 5 min. Lysates were collected and subjected to serial immunoprecipitations, first using anti-TNFR1 antibodies, and then after eluting under denaturing (6 M urea) conditions secondary immunoprecipitations were performed using linkage-specific anti-ubiquitin antibodies (anti-K11, anti-K48, anti-K63). Input lysates, left panel, were analysed by western blot with anti-RIP1, anti-IκBα, and anti-c-IAP1 antibodies. Serially immunoprecipitated material, right panel, was detected using anti-RIP1 antibody. (**B**) Time course of K11-linked polyubiquitination of RIP1 following TNFα stimulation. HeLa S3 cells were treated as in panel (**A**), except additional 20 and 45 min time points were included. Serial immunoprecipitations and western blot analysis were performed as in (**A**), using the indicated antibodies. (**C**) K11-linked polyubiquitination of RIP1 is dependent on c-IAP1. HeLa S3 cells were pretreated with or without 3 μM IAP antagonist (BV6) for 15 h, followed by treatment with 20 μM MG132 for 10 min, and then incubation with or without 100 ng/ml TNFα for 5 min. Serial immunoprecipitations and western blot analysis were performed as in (**A**), using the indicated antibodies. (**D**) K11-linked polyubiquitination of RIP1 involves the UbcH5 family of E2 enzymes. HeLa S3 cells were transfected with control siRNA, or siRNA targeting the UbcH5 family, Ube2S, or UbcH13. At 48 h later, cells were pretreated with 20 μM MG132 for 10 min, and then incubated with or without 100 ng/ml TNFα for 5 min. Lysates were prepared in lysis buffer containing 6 M urea, diluted and immunoprecipitated using the anti-K11-linkage-specific antibody. siRNA knockdown efficiency was analysed by western blot analysis of input lysates, right panel, using the following antibodies: anti-RIP1, anti-UbcH5, anti-UbcH13, anti-Ube2S, and anti-actin, as a loading control. Ubiquitinated endogenous RIP1, right panel, was detected in the immunoprecipitated material using an anti-RIP1 antibody.

the overall protein structure. The functional relevance of these interactions was examined by knockdown of E2 enzymes that interacted with c-IAP1. In these experiments, loss of the UbcH5 family showed a significant impact on c-IAP1 stability, as well on the stability and ubiquitination status of c-IAP1 substrates NIK and RIP1. Knockdown of the other IAP RING domain-binding E2 enzymes identified in the yeast

two-hybrid screen did not impact the stability of c-IAP1, or of its substrates.

However, it is possible that c-IAP proteins have important roles in other, yet unidentified, biological processes and that interactions with ubiquitin-conjugating enzymes identified herein may have substantial physiological importance. One such example is Ube2S, an E2 enzyme with a critical role in
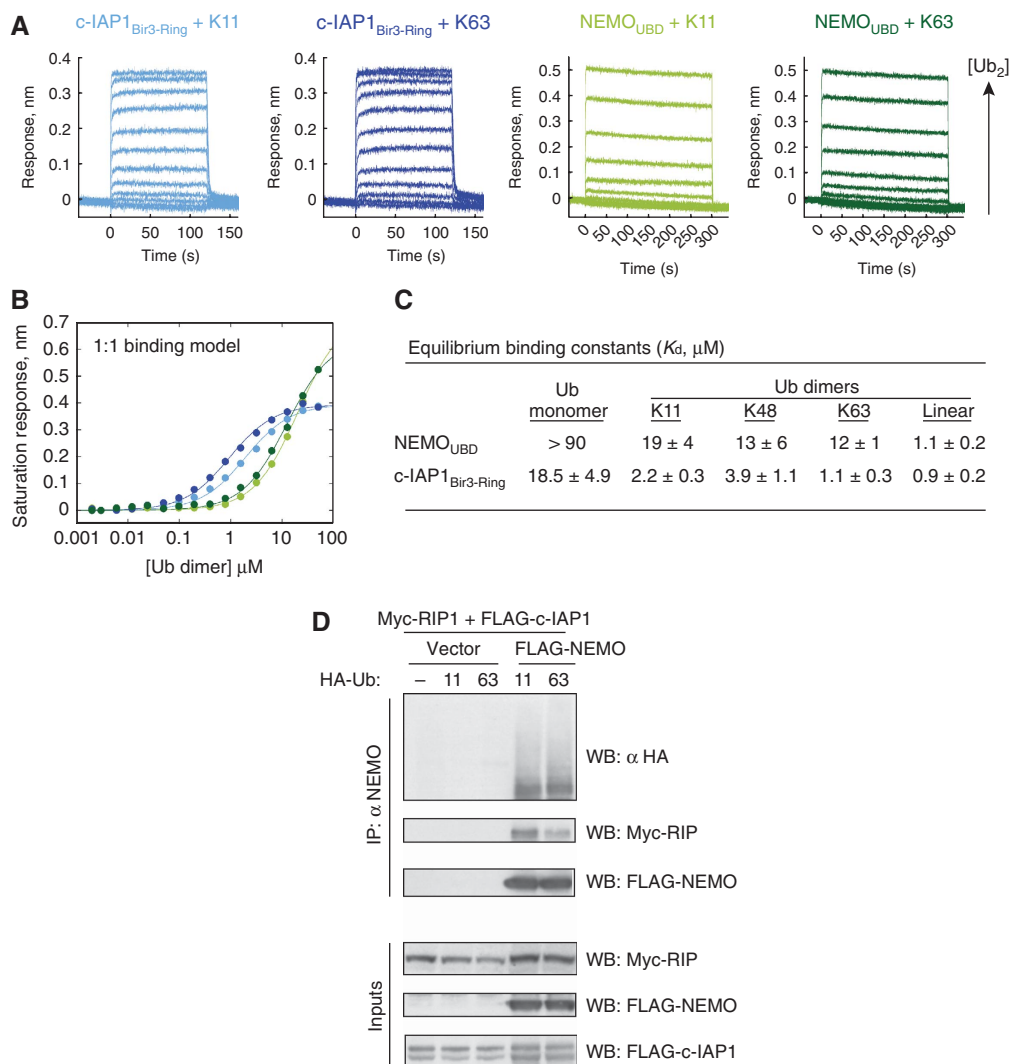
Figure 6 NEMO binds K11-linked ubiquitin chains. Ub binding measured by biolayer interferometry (**A–D**). (**A**) Direct binding of biotinylated NEMO$_{UBD}$ and c-IAP1$_{BIR3-RING}$ to K11- and K63-linked ubiquitin dimers are shown as raw sensograms (response in nm plotted as a function of time) for a range of ubiquitin dimer concentrations. (**B**) Saturation response values from the sensograms in (**A**) are plotted as a function of ubiquitin dimer concentration. The resulting binding curves were fit to a simple 1:1 binding model to determine equilibrium-binding constants (K_d). (**C**) A summary of the determined K_d values is shown with s.d. ($n = 3$). (**D**) NEMO binds K11-linked ubiquitin chains *in vivo*. 293T cells were transfected with Myc-RIP1, FLAG-c-IAP1, HA-tagged ubiquitin constructs (K11- or K63-only), and with or without FLAG-NEMO for 40 h. Protein samples were immunoprecipitated using anti-NEMO antibodies and western blotting of cellular lysates and immunoprecipitates was performed with the indicated antibodies.

cell-cycle regulation and a preference for building K11-linked polyubiquitin chains. Ube2S generally cannot assemble ubiquitin chains on a substrate by itself, but it can serve as an extending enzyme after another E2 has initiated ubiquitin chain formation (Garnett *et al*, 2009; Williamson *et al*, 2009). In our reconstituted ubiquitination assay, Ube2S promoted c-IAP1 ubiquitination, suggesting that the c-IAP ubiquitin ligases might rely on initiating and extending E2 enzymes for fine-tuning the assembly of complex polyubiquitin chains. In addition, some E2 enzymes, like RAD6B and UBE2Q2, have close homologous that could provide functional redundancy in cellular assays (Michelle *et al*, 2009).

Polyubiquitin chains that are formed through different lysine residue linkages adopt distinct structural conformations, thus allowing these posttranslational modifications to regulate a diverse array of cellular processes (Newton *et al*, 2008; Komander, 2009; Bremm *et al*, 2010; Matsumoto *et al*,

2010; Virdee *et al*, 2010). For example, K63-linked polyubiquitin chains were believed to be instrumental for the recruitment of NEMO and for NF-κB activation by TNFα. However, recent reports have shown that c-IAP proteins can promote both K48- and K63-linked ubiquitination of RIP1, and that K63-linked ubiquitin chains are not essential for TNF signalling (Bertrand *et al*, 2008; Varfolomeev *et al*, 2008; Xu *et al*, 2009). In addition, NEMO displays even higher affinity for the newly discovered linear ubiquitin chains (Lo *et al*, 2009; Rahighi *et al*, 2009). Thus, the plasticity of the TNFR1-associated signalling complex permits a signalling role for a multitude of ubiquitin chain linkages. In this study, we demonstrate for the first time that K11-linked polyubiquitin chains may have a function in TNF signalling. Previously, K11-linked ubiquitin chains were characterized as degradative signals in cell-cycle regulation (Kirkpatrick *et al*, 2006; Jin *et al*, 2008; Garnett *et al*, 2009; Williamson *et al*, 2009).

It is still possible that K11-linked ubiquitin chains might contribute to RIP1 degradation. However, their presence in the TNFR1 complex and the ability of NEMO to bind K11-, K48-, and K63-linked ubiquitin chains with comparable affinities suggests that K11-linked ubiquitin chains should also have a signalling role.

As ubiquitination is such an integral component of TNF signalling, many proteins have been (somewhat arbitrarily) ascribed more, or less, prominent roles in this process. Our study provides evidence that the c-IAP proteins and the UbcH5 family of E2 enzymes have a crucial role in RIP1 ubiquitination in the context of TNF signalling while UbcH13 does not. Using linkage-specific anti-ubiquitin antibodies we demonstrate that c-IAP1 is critical for the assembly of all tested ubiquitin linkages on RIP1 in the TNFR1 complex, which is in agreement with the seminal role of c-IAP proteins in TNFR1-mediated signalling (Bertrand *et al*, 2008; Mahoney *et al*, 2008; Varfolomeev and Vucic, 2008; Varfolomeev *et al*, 2008). As small-molecule antagonists of IAP proteins advance in clinical trials for the treatment of cancer (Fulda, 2007), it will be increasingly important to establish the role of IAP proteins in various signalling pathways that regulate cellular proliferation and homeostasis.

Materials and methods

Directed yeast two-hybrid screens
The construction of IAP RING domain-containing bait plasmids is described in the supporting Supplementary data. The E2 library constructs, in the pACT2 prey vector, were kindly provided by Rachel Klevit. The yeast strain AH109 (Clontech) was co-transformed with respective bait and prey plasmids and positive transformants were selected on minimal SD–Leu–Trp medium (Clontech). Two single colonies for each bait and prey co-transformation were suspended in 100 μl of phosphate-buffered saline and then replica plated onto non-selective (SD–Leu–Trp) or selective medium (SD–His–Leu–Trp, plus 0, 2.5, 5, 10, or 20 mM 3-amino-1,2,4-triazole (3AT; Sigma). Yeast were incubated for 1 week at 30°C.

Cell lines, reagents, and transfections
HEK293T, HeLa S3, HT1080, and HT29 cells were obtained from American Type Culture Collection and maintained in 50:50 RPMI 1640/DMEM medium supplemented with 10% fetal bovine serum (FBS), penicillin and streptomycin. HKB11 cells (from ATCC, an epithelial somatic cell hybrid of kidney and B cells) were transfected with a pIRES-hyg2 (Clontech) plasmid containing the human CD40 receptor, and then the HBK11-CD40 stable cell line was selected with hygromycin. The HBK11-CD40 cell line was maintained in 50:50 RPMI 1640/DMEM medium supplemented with 10% FBS, penicillin, streptomycin, and hygromycin. Human recombinant soluble TNFα, TWEAK, and anti-HER2 antibody (Herceptin) were obtained from Genentech, Inc. Agonistic anti-CD40 antibody was purchased from R&D Systems, and cross-linked with a secondary antibody from Jackson Immunolabs. MG132 was purchased from American Peptide Company. Antibodies against actin (Sigma), Myc (Upstate), Flag (Sigma), HA (Roche), ubiquitin (P4D1, Cell Signaling), RIP1 (BD Biosciences), c-IAP1 (R&D Systems), c-IAP2 (AbCam), XIAP (Cell Signaling), IκBα (Cell Signaling), UbcH5 (Boston Biochem), UbcH13 (ZYMED/Invitrogen), NEMO (R&D), and tsg101 (Genetex) were purchased, and ML-IAP antibody was described previously (Dynek *et al*, 2008). K48- and K63-linkage-specific anti-ubiquitin antibodies were described previously (Newton *et al*, 2008), and a K11-linkage-specific anti-ubiquitin antibody was generated in house (Matsumoto *et al*, 2010). An ultimate ORF clone encoding the full-length Ube2S was purchased from Invitrogen and subcloned into a 6 × His N-terminal Unizyme tagged vector, pST239, expressed in *E. coli* (host cells: 58F3, grown at 30°C in complete C.R.A.P. media overnight), and purified under native conditions over an NiNTA column, followed by purification

over a S-75 gel filtration column. Recombinant full-length Ube2S was used as an antigen for injection, and a polyclonal rabbit antibody was generated and purified by Yenzym antibody, LLC. FLAG-c-IAP1, Myc-RIP1, and ubiquitin mutant constructs were described previously (Varfolomeev *et al*, 2006; Newton *et al*, 2008). c-IAP1 F616A and V573A/D576A, as well as UbcH5b siRNA-resistance mutations were introduced using QuikChange site-directed mutagenesis kit (Stratagene). HEK293T transient transfections were done using Geneporter 2 reagent (Genlantis). HeLa S3 and HT1080 cells were transfected with siRNA oligonucleotides using Lipofectamine RNAiMAX (Invitrogen); siRNA sequences are included in the supporting Supplementary data.

Western blot analysis and immunoprecipitation
Western blot analyses were performed as described previously (Vucic *et al*, 2002). For immunoprecipitation of FLAG-c-IAP1 and myc-RIP1, cells were lysed in NP40 lysis buffer (1% NP40, 150 mM NaCl, 50 mM Tris (pH 7.5), 1 mM DTT, and protease inhibitor cocktail (Roche)), precleared with protein A/G agarose (Pierce) and incubated with anti-FLAG (Sigma) or anti-myc (Clontech), and immunoprecipitations carried out as described previously (Vucic *et al*, 2002). Immunoprecipitation of receptor-bound RIP1 was done as described previously (Newton *et al*, 2008), except using monoclonal anti-TNFR1 antibodies from R&D Systems for the primary immunoprecipitation, and K11-linkage-specific anti-ubiquitin antibody for the secondary immunoprecipitation.

Ubiquitination assays and mass spectometry analysis
Ubiquitination reactions with c-IAP1 and RIP1 were performed using reaction components and full-length recombinant c-IAP1 and RIP1 proteins, as described previously (Varfolomeev *et al*, 2007, 2008; Blankenship *et al*, 2009). Recombinant c-IAP2 protein was purchased from R&D; UbcH5 a, b, and c as well as wild type and mutant versions of ubiquitin were purchased from Boston Biochem. Following ubiquitination reactions, samples were incubated in 6 M urea at room temperature for 30 min with rocking, diluted 15 times and immunoprecipitated using anti-RIP1 antibodies. Ubiquitination reactions were analysed by the Ubiquitin-AQUA method using LTQ-OrbiTrap as described in Supplementary data.

Reconstituted c-IAP1 auto-ubiquitination assays were performed as described previously (Varfolomeev *et al*, 2007; Blankenship *et al*, 2009) using 2 μg E2 (UbcH5a or Ube2S) and 2 μg of c-IAP1 with the following modifications: reactions were first incubated at 21°C for 5 min with or without 0.1 μg of UbcH5a (first step), followed by the addition of the indicated E2 enzymes and subsequent incubation for an additional 35 min at 37°C (second step). The reactions were stopped by adding 4 × LDS loading buffer, boiled at 90°C for 10 min and resolved on SDS–PAGE. Ubiquitination reactions were analysed by the Ubiquitin-AQUA method with multiple reaction monitoring on a QTrap4000 (Applied Biosystems) mass spectrometer as described previously (Kirkpatrick *et al*, 2006; Blankenship *et al*, 2009). The area of each analyte and internal standard peak was used to determine the abundance of each peptide in the sample. Total ubiquitin abundance was determined as the average of values quantified from the K11, K33, K48, and K63 loci.

Ubiquitin-binding assays
Binding to ubiquitin monomer and ubiquitin dimers of varying linkages was measured by biolayer interferometry on an Octet RED384 instrument (ForteBio, Inc.). Biotinylated NEMO$_{UBD}$ or c-IAP1$_{BIR3-RING}$ stocks were captured onto streptavidin SA biosensors at 20–40 μg/ml and washed to remove any unbound material before conducting association and dissociation measurements with discrete ubiquitin analytes in GF Buffer (composition in the Supplementary data) supplemented with 0.1 mg/ml BSA and 0.02% Tween-20. The interactions monitored displayed rapid saturation behaviour and thus were ideally evaluated by equilibrium-binding analysis in which saturation response (nm) was plotted as a function of ubiquitin analyte concentration using a simple 1:1 binding equation using Kaleidagraph version 3.6 (Synergy Software):

$$R = (R_{max}) \times ([A]_T / (K_d + [A]_T)),$$

where R is the response value, R_{max} is the maximal response, $[A]_T$ is the total ubiquitin analyte concentration, and K_d is the equilibrium dissociation constant. Binding assays were performed in triplicate and the average K_d values were reported with standard deviations.

Conflict of interest

All authors are employees of Genentech, Inc.

References

Bertrand MJ, Milutinovic S, Dickson KM, Ho WC, Boudreault A, Durkin J, Gillard JW, Jaquith JB, Morris SJ, Barker PA (2008) cIAP1 and cIAP2 facilitate cancer cell survival by functioning as E3 ligases that promote RIP1 ubiquitination. *Mol Cell* **30:** 689–700

Blankenship JW, Varfolomeev E, Goncharov T, Fedorova AV, Kirkpatrick DS, Izrael-Tomasevic A, Phu L, Arnott D, Aghajan M, Zobel K, Bazan JF, Fairbrother WJ, Deshayes K, Vucic D (2009) Ubiquitin binding modulates IAP antagonist-stimulated proteasomal degradation of c-IAP1 and c-IAP2. *Biochem J* **417:** 149–160

Bremm A, Freund SM, Komander D (2010) Lys11-linked ubiquitin chains adopt compact conformations and are preferentially hydrolyzed by the deubiquitinase Cezanne. *Nat Struct Mol Biol* **17:** 939–947

Christensen DE, Brzovic PS, Klevit RE (2007) E2-BRCA1 RING interactions dictate synthesis of mono- or specific polyubiquitin chain linkages. *Nat Struct Mol Biol* **14:** 941–948

Deshaies RJ, Joazeiro CA (2009) RING domain E3 ubiquitin ligases. *Annu Rev Biochem* **78:** 399–434

Dynek JN, Chan SM, Liu J, Zha J, Fairbrother WJ, Vucic D (2008) Microphthalmia-associated transcription factor is a critical transcriptional regulator of melanoma inhibitor of apoptosis in melanomas. *Cancer Res* **68:** 3124–3132

Ea CK, Deng L, Xia ZP, Pineda G, Chen ZJ (2006) Activation of IKK by TNFalpha requires site-specific ubiquitination of RIP1 and polyubiquitin binding by NEMO. *Mol Cell* **22:** 245–257

Fulda S (2007) Inhibitor of apoptosis proteins as targets for anticancer therapy. *Expert Rev Anticancer Ther* **7:** 1255–1264

Garnett MJ, Mansfeld J, Godwin C, Matsusaka T, Wu J, Russell P, Pines J, Venkitaraman AR (2009) UBE2S elongates ubiquitin chains on APC/C substrates to promote mitotic exit. *Nat Cell Biol* **11:** 1363–1369

Glickman MH, Ciechanover A (2002) The ubiquitin-proteasome proteolytic pathway: destruction for the sake of construction. *Physiol Rev* **82:** 373–428

Gyrd-Hansen M, Darding M, Miasari M, Santoro MM, Zender L, Xue W, Tenev T, da Fonseca PC, Zvelebil M, Bujnicki JM, Lowe S, Silke J, Meier P (2008) IAPs contain an evolutionarily conserved ubiquitin-binding domain that regulates NF-kappaB as well as cell survival and oncogenesis. *Nat Cell Biol* **10:** 1309–1317

Hershko A, Ciechanover A (1998) The ubiquitin system. *Annu Rev Biochem* **67:** 425–479

Ikeda F, Dikic I (2008) Atypical ubiquitin chains: new molecular signals. 'Protein modifications: beyond the usual suspects' review series. *EMBO Rep* **9:** 536–542

Jin L, Williamson A, Banerjee S, Philipp I, Rape M (2008) Mechanism of ubiquitin-chain formation by the human anaphase-promoting complex. *Cell* **133:** 653–665

Kirkpatrick DS, Hathaway NA, Hanna J, Elsasser S, Rush J, Finley D, King RW, Gygi SP (2006) Quantitative analysis of *in vitro* ubiquitinated cyclin B1 reveals complex chain topology. *Nat Cell Biol* **8:** 700–710

Komander D (2009) The emerging complexity of protein ubiquitination. *Biochem Soc Trans* **37:** 937–953

Kovalenko A, Wallach D (2006) If the prophet does not come to the mountain: dynamics of signaling complexes in NF-kappaB activation. *Mol Cell* **22:** 433–436

Li H, Kobayashi M, Blonska M, You Y, Lin X (2006) Ubiquitination of RIP is required for tumor necrosis factor alpha-induced NF-kappaB activation. *J Biol Chem* **281:** 13636–13643

Lo YC, Lin SC, Rospigliosi CC, Conze DB, Wu CJ, Ashwell JD, Eliezer D, Wu H (2009) Structural basis for recognition of diubiquitins by NEMO. *Mol Cell* **33:** 602–615

Mace PD, Linke K, Feltham R, Schumacher FR, Smith CA, Vaux DL, Silke J, Day CL (2008) Structures of the cIAP2 RING domain reveal conformational changes associated with ubiquitin-conjugating enzyme (E2) recruitment. *J Biol Chem* **283:** 31633–31640

Mahoney DJ, Cheung HH, Mrad RL, Plenchette S, Simard C, Enwere E, Arora V, Mak TW, Lacasse EC, Waring J, Korneluk RG (2008) Both cIAP1 and cIAP2 regulate TNFalpha-mediated NF-kappaB activation. *Proc Natl Acad Sci USA* **105:** 11778–11783

Matsumoto ML, Wickliffe KE, Dong KC, Yu C, Bosanac I, Bustos D, Phu L, Kirkpatrick DS, Hymowitz SG, Rape M, Kelley RF, Dixit VM (2010) K11-linked polyubiquitination in cell cycle control revealed by a K11 linkage-specific antibody. *Mol Cell* **39:** 477–484

Michelle C, Vourc'h P, Mignon L, Andres CR (2009) What was the set of ubiquitin and ubiquitin-like conjugating enzymes in the eukaryote common ancestor? *J Mol Evol* **68:** 616–628

Newton K, Matsumoto ML, Wertz IE, Kirkpatrick DS, Lill JR, Tan J, Dugger D, Gordon N, Sidhu SS, Fellouse FA, Komuves L, French DM, Ferrando RE, Lam C, Compaan D, Yu C, Bosanac I, Hymowitz SG, Kelley RF, Dixit VM (2008) Ubiquitin chain editing revealed by polyubiquitin linkage-specific antibodies. *Cell* **134:** 668–678

Pickart CM, Fushman D (2004) Polyubiquitin chains: polymeric protein signals. *Curr Opin Chem Biol* **8:** 610–616

Rahighi S, Ikeda F, Kawasaki M, Akutsu M, Suzuki N, Kato R, Kensche T, Uejima T, Bloor S, Komander D, Randow F, Wakatsuki S, Dikic I (2009) Specific recognition of linear ubiquitin chains by NEMO is important for NF-kappaB activation. *Cell* **136:** 1098–1109

Rothe M, Pan MG, Henzel WJ, Ayres TM, Goeddel DV (1995) The TNFR2-TRAF signaling complex contains two novel proteins related to baculoviral inhibitor of apoptosis proteins. *Cell* **83:** 1243–1252

Salvesen GS, Duckett CS (2002) IAP proteins: blocking the road to death's door. *Nat Rev Mol Cell Biol* **3:** 401–410

Scheidereit C (2006) IκB kinase complexes: gateways to NF-κB activation and transcription. *Oncogene* **25:** 6685–6705

Schulman BA, Harper JW (2009) Ubiquitin-like protein activation by E1 enzymes: the apex for downstream signalling pathways. *Nat Rev Mol Cell Biol* **10:** 319–331

Varfolomeev E, Blankenship JW, Wayson SM, Fedorova AV, Kayagaki N, Garg P, Zobel K, Dynek JN, Elliott LO, Wallweber HJ, Flygare JA, Fairbrother WJ, Deshayes K, Dixit VM, Vucic D (2007) IAP antagonists induce autoubiquitination of c-IAPs, NF-κB activation, and TNFα-dependent apoptosis. *Cell* **131:** 669–681

Varfolomeev E, Goncharov T, Fedorova AV, Dynek JN, Zobel K, Deshayes K, Fairbrother WJ, Vucic D (2008) c-IAP1 and c-IAP2 are critical mediators of tumor necrosis factor alpha (TNFα)-induced NF-κB activation. *J Biol Chem* **283:** 24295–24299

Varfolomeev E, Vucic D (2008) (Un)expected roles of c-IAPs in apoptotic and NF-κB signaling pathways. *Cell Cycle* **7:** 1511–1521

Varfolomeev E, Wayson SM, Dixit VM, Fairbrother WJ, Vucic D (2006) The inhibitor of apoptosis protein fusion c-IAP2.MALT1

stimulates NF-κB activation independently of TRAF1 AND TRAF2. *J Biol Chem* **281:** 29022–29029

Vaux DL, Silke J (2005) IAPs, RINGs and ubiquitylation. *Nat Rev Mol Cell Biol* **6:** 287–297

Vince JE, Wong WW, Khan N, Feltham R, Chau D, Ahmed AU, Benetatos CA, Chunduru SK, Condon SM, McKinlay M, Brink R, Leverkus M, Tergaonkar V, Schneider P, Callus BA, Koentgen F, Vaux DL, Silke J (2007) IAP antagonists target cIAP1 to induce TNFalpha-dependent apoptosis. *Cell* **131:** 682–693

Virdee S, Ye Y, Nguyen DP, Komander D, Chin JW (2010) Engineered diubiquitin synthesis reveals Lys29-isopeptide specificity of an OTU deubiquitinase. *Nat Chem Biol* **6:** 750–757

Vucic D, Deshayes K, Ackerly H, Pisabarro MT, Kadkhodayan S, Fairbrother WJ, Dixit VM (2002) SMAC negatively regulates the anti-apoptotic activity of melanoma inhibitor of apoptosis (ML-IAP). *J Biol Chem* **277:** 12275–12279

Wang CY, Mayo MW, Korneluk RG, Goeddel DV, Baldwin Jr AS (1998) NF-κB antiapoptosis: induction of TRAF1 and TRAF2 and c-IAP1 and c- IAP2 to suppress caspase-8 activation. *Science* **281:** 1680–1683

Williamson A, Wickliffe KE, Mellone BG, Song L, Karpen GH, Rape M (2009) Identification of a physiological E2 module for the human anaphase-promoting complex. *Proc Natl Acad Sci USA* **106:** 18213–18218

Wu CJ, Conze DB, Li T, Srinivasula SM, Ashwell JD (2006) Sensing of Lys 63-linked polyubiquitination by NEMO is a key event in NF-kappaB activation. *Nat Cell Biol* **8:** 398–406

Xu M, Skaug B, Zeng W, Chen ZJ (2009) A ubiquitin replacement strategy in human cells reveals distinct mechanisms of IKK activation by TNFalpha and IL-1beta. *Mol Cell* **36:** 302–314

Yang QH, Du C (2004) Smac/DIABLO selectively reduces the levels of c-IAP1 and c-IAP2 but not that of XIAP and livin in HeLa cells. *J Biol Chem* **279:** 16963–16970

Yin Q, Lamothe B, Darnay BG, Wu H (2009a) Structural basis for the lack of E2 interaction in the RING domain of TRAF2. *Biochemistry* **48:** 10558–10567

Yin Q, Lin SC, Lamothe B, Lu M, Lo YC, Hura G, Zheng L, Rich RL, Campos AD, Myszka DG, Lenardo MJ, Darnay BG, Wu H (2009b) E2 interaction and dimerization in the crystal structure of TRAF6. *Nat Struct Mol Biol* **16:** 658–666